

Free radical polymerization in multilaminated microreactors: 2D and 3D multiphysics CFD modeling

Christophe Serra · Guy Schlatter · Nicolas Sary ·
Friedhelm Schönfeld · Georges Hadziioannou

Received: 1 July 2006 / Accepted: 25 September 2006 / Published online: 16 December 2006
© Springer-Verlag 2006

Abstract This paper investigates the modeling of styrene free radical polymerization in two different types of microreactor. A multiphysics model which simultaneously takes into account the hydrodynamics, thermal and mass transfer (convection, diffusion and chemical reaction) is proposed. The set of partial differential equations resulting from the model is solved with the help of the finite elements method either in a 2D or a 3D approach. The different modeled microreactors are on one hand an interdigital multilamination microreactor with a large focusing section, and on the other hand a simple T-junction followed by a straight tube with three different radii. The results are expressed in terms of reactor temperature, polydispersity index, number-average degree of polymerization and monomer conversion for different values of the chemical species diffusion coefficient. It was found that the 2D approach gives the same results as the 3D approach but allows to dramatically reduce the computing time. Despite the heat released by the polymerization reaction, it was found that the thermal transfer in such microfluidic devices is high enough to ensure isothermal conditions. Concerning the polydispersity index, the range of diffusion coefficients over which the polydispersity index can be maintained close to the theoretical

value for ideal conditions increases as the tube reactor radius decreases. The interdigital multilamination microreactor was found to act as a tubular reactor of 0.78 mm ID but with a shorter length. This underlines that the use of microfluidic devices can lead to a better control of polymerization reactions.

Keywords Numerical simulation · Free radical polymerization · Microreactor · Modeling

List of symbols

Acronyms

PDI	Polydispersity index
RTD	Residence time distribution
SFIMM	Superfocus interdigital multilamination micromixer
ST	Straight tube section of the tubular reactor
TJ	T-junction section of the tubular reactor
TR	Tubular reactor

Symbol descriptions

a	scaling factor
C_i	concentration of specie i (mol/l)
C_{I0}	initial initiator concentration (mol/l)
C_{M0}	initial monomer concentration (mol/l)
C_p	fluid heat capacity (J/kg/K)
D_i	diffusion coefficient of specie i (m ² /s)
DP_n	number-average degree of polymerization
f	initiator efficiency
k	fluid thermal conductivity (W/m/K)
k_d	kinetic constant of the initiator decomposition (1/s)
k_p	kinetic constant of the propagation reaction (l/mol/s)

C. Serra (✉) · G. Schlatter · N. Sary · G. Hadziioannou
Laboratoire d'Ingénierie des Polymères pour les Hautes
Technologies, CNRS UMR 7165, ECPM—ULP Strasbourg,
25 rue Becquerel, Strasbourg Cedex 2 67087, France
e-mail: SerraC@ecpm.u-strasbg.fr

F. Schönfeld
Institut für Mikrotechnik Mainz GmbH,
Carl-Zeiss-Str. 18-20, Mainz 55129, Germany

k_{tc}	kinetic constant of the termination reaction (l/mol/s)
L	kinetic chain length or reactor length (m)
L_{ST}	ST length (m)
L_{TJ}	TJ length (m)
p	pressure (Pa)
Pe_R	radial Peclet number
Pe_L	axial Peclet number
Q	Heat source (W/m ³)
R_i	rate of production of specie i (mol/l/s)
R	tubular reactor radius (m)
t	time (s)
t'	pseudo time (s)
T	temperature (K)
\mathbf{u}	velocity vector (m/s)
W_0	SFIMM channel width (m)
X_M	monomer conversion
ΔH_p	enthalpy of the propagation reaction (J/mol)

Greek symbols

η	viscosity of fluid (Pa.s)
λ_i	i th moment of the living polymer distribution (mol/l)
μ_i	i th moment of the dead polymer distribution (mol/l)
μ_i'	normalized i th moment of the dead polymer distribution -
ρ	density of fluid (kg/m ³)
τ	residence time (s)

Chemical species

I	Initiator
M	Monomer
P_n	Dead polymer of chain length n
P_n^*	Living polymer of chain length n
P^*	Overall living polymer (whatever the chain length)
R^*	Primary radicals

1 Introduction

Microfluidic devices are now widely used in chemical and biochemical analysis systems (μ TAS) since they require a very small quantity of the sample to be analyzed and can considerably speed up the analysis process (Geschke et al. 2004). Their use is also growing in other scientific fields like chemical engineering and polymer science. Indeed their high wall surface-to-volume ratio as well as their small characteristic length enhance thermal and mass transport which make them suitable for the study and control of highly exothermic,

fast and mass-limited chemical reactions (Hisamoto et al. 2001; Hessel et al. 2004, 2005; Hessel and Löwe 2005). If in the specific area of polymer particles synthesis the use of microfluidic devices is booming, quite a few studies are reported concerning the continuous synthesis of polymer through bulk or solution processes in such devices. However, polymerizations reactions can really benefit from the high degree of mixing achieved in micromixers. Thus, Bayer et al. (2000) investigated the free radical polymerization of acrylic resins. They showed that the use of micromixers can avoid the fouling observed in conventional static mixers for this process. Anionic (Honda et al. 2005; Miyazaki et al. 2006) and cationic (Nagaki et al. 2004) polymerizations were also studied. Since these polymerization techniques are characterized by extremely high initiation and propagation rates, the mixing of the reagents is a critical issue. The use of a micromixer prior to the polymerization was found to significantly reduce the molecular weight distribution of the synthesized polymers. Mixing is also a critical issue for reaction pathways which lead to unwanted side reactions when gradients of reactants' concentration occur. Thus, Liu et al. (2006) have shown that the use of an interdigital micromixer can reduce the time required to obtain a "full generation" of a poly(amidoamine) dendrimer (PANAM), synthesized from an ethylenediamine core (EDA) and methyl acrylate precursor, to only 3 s. In conventional batch reactors, one should operate with a large excess of EDA to avoid an intramolecular amidation side reaction resulting in a long-time reaction: 96 h to obtain the "full generation". In the continuous two-stage nitroxide-mediated poly(-butyl acrylate)-b-poly(styrene) copolymerization, Rosenfeld et al. (2006a) have shown that an interdigital micromixer can significantly help to lower the overall copolymer polydispersity down to 1.4 by efficiently mixing the first viscous block poly(butyl acrylate) with the liquid comonomer (styrene). When a simple T-junction was used instead of the micromixer, the copolymer's polydispersity was found quite higher and equal to 1.73. Polymerization reactions can also benefit from the fast heat transfer encountered in microreactors. Iwasaki and Yoshida (2005) and Rosenfeld et al. (2006b) reported, respectively, free radical polymerization and Nitroxide-mediated radical polymerization reactions in microtube reactors of, respectively, 500 and 900 μ m internal diameters. Both authors have shown that the use of small reactor dimensions did not lead to significantly different results from standard lab-scale reactors for low exothermic monomers like styrene or vinyl benzoate. However, for highly exothermic monomers like butyl acrylate, the molecular

weight distribution was found quite narrower than for the batchwise system. They claimed that it comes directly from the high surface-to-volume ratio of the microtube reactor which allows a better removal of the heat released by the polymerization. Another advantage of microfluidic devices is the ability to rapidly generate libraries of polymer materials. Thus, the use of a microchannel reactor with multiple entries allows the synthesis of polymers (Wu et al. 2004; Cabral et al. 2004) and copolymers (Wu et al. 2005) with different molecular weights and compositions by simply varying the flow rate ratios in-between the different reagents.

All these studies suggest that microtubes and micromixers can significantly improve the control of polymerization reactions; the former by allowing a rapid removal of the heat released by the polymerization and the latter by promoting an efficient mixing of the reactants. A microfluidic device combining both advantages will be probably of much help in controlling all types of polymerization reactions. This can be obtained by considering that the polymerization is directly performed inside the micromixer. Here, we want to investigate the capacity of an interdigital micromixer in controlling the semi-diluted (30% solvent) styrene free radical homopolymerization as opposed to a tubular reactor with different radii. The investigations are conducted through the modeling of the polymerization in these two microreactors with the help of a multiphysics CFD software package.

2 Microreactors

Two different types of microreactors have been studied (cf. Fig. 1). The first one, commercialized by the IMM Company (Mainz, Germany), is the SuperFocus Interdigital Multilamination Micromixer (SFIMM). The second one is a tubular reactor (TR) comprising two sections: a T-junction (TJ) with different radii (0.24/1/5 mm) and 14 mm length followed by a straight tube

(ST) with the same radius (0.24/1/5 mm). The length of the ST section is fixed to keep the volume equal to that of the SFIMM. The TJ section brings together all the reagents and is kept at a low temperature to avoid the polymerization start, whereas the ST section is the locus of the polymerization reaction. All devices' characteristics are given in Table 1.

The SFIMM uses the principle of interdigital multilamination and geometrical focusing. The two inlet flows are distributed in staggered rows along an arc containing 138 small inlet channels of 250 μm thickness. Then, the fluids are focused in a delta-shaped section before entering the mixing section consisting of a 500 μm wide straight exit channel where the fluid lamellae have an average thickness of 4 μm . However, in this study, the SFIMM is considered as a microreactor. Therefore, the focusing section (cf. Fig. 1a) will be the locus of the polymerization reaction as well as of the diffusional mixing of the reagents enabled by the low flowrates of these reagents. It is then supposed that only the focusing section is heated to promote the polymerization reaction and that the so-called mixing section (cf. Fig. 1a) is cooled down to quench the reaction.

On the other hand, under sufficiently high Reynolds numbers, T-junctions can act as quite efficient micromixers (Wong et al. 2004). The 'stratified' flow with low interfaces for mixing and diffusion then changes to an entangled, so-called 'vortex' flow with highly stretched interfaces and convection supporting diffusion as the mixing mechanism. Besides flow velocity, simple parameters such as flow direction or flow ratio can also have a significant impact on the mixing efficiency.

One should note that these microfluidic devices can all be considered like lamination devices. Indeed at low Reynolds numbers the TJ operates like a bilamination micromixer as compared with SFIMM. Moreover, the TR + ST and SFIMM microreactors are characterized by a large focusing section. Thus, the study of these two microreactor devices will allow

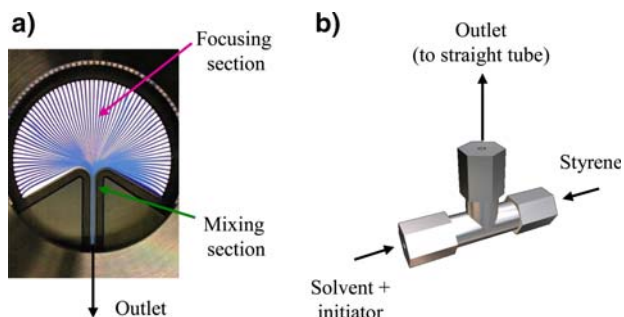


Fig. 1 Microreactors considered: **a** SFIMM (courtesy of IMM), **b** TJ + ST (not represented)

Table 1 Devices' characteristics

	SFIMM	TR 0.24	TR 1	TR 5
Tube radius (mm)	–	0.24	1	5
Tube length (mm)	15	22,405	1,252	50
Height (mm)	5	–	–	–
Channel width (mm)	0.25	–	–	–
Fin width (mm)	0.361	–	–	–
Channel number	138	–	–	–
Contact area/volume (m^{-1}) ^a	2,400	2,613	618	124
Wall surface/volume (m^{-1})	400	8,461	2,000	400
Volume (ml)	3.93	3.93	3.93	3.93

^a for immiscible fluids

us to assess the influence of the lamination process on the polymerization result.

3 Model

The geometry of any chemical reactors has a strong influence on (1) the temperature gradient through the thermal conduction/convection phenomena, (2) the residence time distribution (RTD) and pressure loss through the hydrodynamics and (3) the chemicals concentration gradient through the reaction, convection and diffusion of chemical species. Thus, in order to determine which geometry is more appropriate for a microreactor to control the polymerization reactions, we have used a numerical simulation approach based on a model to compare the results in two different geometries.

It is known that in all reactors whatever their geometry and size, there is a strong coupling between all the variables describing the system. Therefore, all the partial differential equations resulting from the hydrodynamics, thermal and mass transfer (convection, diffusion and chemical reaction) have to be solved simultaneously.

These governing equations on the base of which the model is conceived are the continuity equation (1), the momentum conservation (Navier–Stokes) equations (2), the thermal convection–conduction equation (3) and the chemical species convection–conduction equations (4):

$$\nabla \cdot \mathbf{u} = 0 \quad (1)$$

$$\rho \frac{\partial \mathbf{u}}{\partial t} + \rho(\mathbf{u} \cdot \nabla) \mathbf{u} = -\nabla p + \nabla \cdot \left(\eta \left[\nabla \mathbf{u} + (\nabla \mathbf{u})^T \right] \right) \quad (2)$$

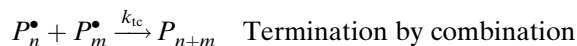
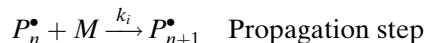
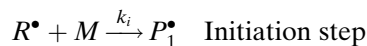
$$\rho C_p \frac{\partial T}{\partial t} + \nabla \cdot (-k \nabla T) = Q - \rho C_p \mathbf{u} \cdot \nabla T \quad (3)$$

$$\frac{\partial C_i}{\partial t} + \nabla \cdot (-D_i \nabla C_i + C_i \mathbf{u}) = R_i \quad (4)$$

where \mathbf{u} denotes the velocity vector, ρ the fluid density, p the pressure, η the fluid viscosity assumed constant, T the temperature, C_p the fluid heat capacity per mass unit assumed constant, k the thermal conductivity assumed constant, Q the heat source per volume unit (the heat released by the polymerization reaction), D_i and C_i , respectively, the diffusion coefficient and concentration of species i and R_i the rate of production of species i .

The heat source and the rate of production depend on the studied polymerization. Here, the styrene free

radical polymerization was studied for which a simplified kinetic scheme may be represented as follows:



where I is the initiator, R^\bullet the primary radicals, M the monomer (styrene), P_n^\bullet the living polymers of chain length n , P_n the dead polymers of chain length n and k_x the kinetic constants of the different reactions (Chen 1998).

Considering that the propagation step contributes mainly to the heat released by the polymerization, the heat source is given by:

$$Q = -\Delta H_p k_p C_p C_M \quad (5)$$

where ΔH_p is the enthalpy of the propagation reaction and P^\bullet the living polymers (whatever the chain length).

Introducing the zeroth, first and second moment of the number chain length distribution (NCLD) of the living and dead polymers (respectively, λ_0 , λ_1 , λ_2 , and μ_0 , μ_1 , μ_2),

$$\lambda_j = \sum_{n=1}^{\infty} n^j C_{P_n} \quad (6)$$

$$\mu_j = \sum_{n=1}^{\infty} n^j C_{P_n} \quad (7)$$

the rate of production of the different species of interest can be expressed by (Villermaux et al. 1983; Dostson et al. 1996; Iedema et al. 2003):

$$R_I = -k_d C_I \quad (8)$$

$$R_M = -k_p \lambda_0 C_M \quad (9)$$

$$R_{\mu_0} = \frac{1}{2} k_{tc} \lambda_0^2 \quad (10)$$

$$R_{\mu_1} = k_{tc} \lambda_0 \lambda_1 \quad (11)$$

$$R_{\mu_2} = k_{tc} (\lambda_0 \lambda_2 + \lambda_1^2). \quad (12)$$

By applying the quasi steady state approximation (QSSA), the moments of the living polymer number chain length distribution are given by:

$$\lambda_0 = C_{P^*} = \sqrt{\frac{2k_d f C_I}{k_{tc}}} \tag{13}$$

$$\lambda_1 = L\lambda_0 \tag{14}$$

$$\lambda_2 = 2\lambda_0 L^2 \tag{15}$$

where L is the kinetic chain length and f the initiator efficiency supposed to be equal to 1 (Chen 1998).

$$L = \frac{k_p \lambda_0 C_M}{2k_d f C_I} \tag{16}$$

Finally, the polydispersity index (PDI), the number-average degree of polymerization (DP_n) and the monomer conversion (X_M) are expressed by the following three equations:

$$PDI = \frac{\mu_0 \mu_2}{\mu_1^2} \tag{17}$$

$$DP_n = \frac{\mu_1}{\mu_0} \tag{18}$$

$$X_M = \frac{C_{M0} - C_M}{C_{M0}} \tag{19}$$

where C_{M0} is the initial monomer concentration.

The moments calculated thanks to Eqs. (10) to (12) are separated by several orders of magnitude. To reduce the stiffness of the system and thus, to ensure the convergence, we have introduced the following modified moments (Zhu 1999):

$$\mu'_0 = \mu_0 / C_{I0} \tag{20}$$

$$\mu'_1 = \mu_1 / C_{M0} \tag{21}$$

$$\mu'_2 = \mu_2 / (C_{M0}^2 / C_{I0}) \tag{22}$$

where C_{I0} is the initial initiator concentration.

4 Numerical simulations: 2D and 3D approaches

Equations (1–4) have been solved with the help of finite elements method by using Femlab 3.1 software (Comsol AB) running on a personal computer. Two sets of simulations were performed: either using 3D or 2D meshes.

4.1 3D simulations

The first set of simulation was performed with a 3D mesh representing each microreactor. Due to its

circular geometry, it is expected that the streamlines of the SFIMM are straight from the periphery to the center of the focusing section. For that reason, the simulations were performed only on a trapezoidal cut of the focusing section (cf. Fig. 1). This trapezoidal cut represents a repetitive unit of the focusing section, comprising half of a channel (125 μm width) for each reagent plus the wall (360 μm width) in between the two channels.

In order to reduce the memory required to run the simulations and by taking into account the symmetry of the microreactors' geometry, the mesh was made (cf. Fig. 2) on a) the trapezoidal cut of the SFIMM, b) half of the TJ and c) half of the ST. Refinement was made where the reagents are put together since strong changes in their concentrations are likely to occur.

Depending on the ST radius, the length to radius ratio ranges from 10 to 94,781 (!). Therefore, the mesh is highly stretched in the z direction. Thus, to enhance the numerical quality of finite elements without increasing their number, a change of the scale was done in the z direction by introducing the following relationship:

$$z' = az \tag{23}$$

where a is a scaling factor. This leads to the modification of each derivative regarding to z for Eqs. (1–4). A minimum value of $a = 10^{-4}$ had to be taken because of the loss of the conditioning of the numerical system.

4.2 2D simulations

A 2D approach has also been developed for the SFIMM and ST geometries. The simplification is based on the consideration of magnitudes of the diffusive fluxes in different spatial directions. For the cases under study (cf. Table 2) we have radial or uniaxial flow profiles. In the case where the axial Peclet number $Pe_L \gg 1$ ($Pe_L = L^2 / \tau D$ where L is the reactor length, τ the mean residence time and D the diffusion coefficient), the axial diffusive term is negligible compared to the axial convective term in Eq. (4).

For the SFIMM geometry we consider a convection–diffusion reaction problem between parallel plates of the trapezoidal cut of the SFIMM as sketched in Fig. 3. The convective term is eliminated by changing to a frame of reference perpendicular to the flow (i.e. r direction). In other words, the residual diffusion, i.e. the diffusion perpendicular to the flow direction, together with the reactive source term is solved on a (xy) rectangular section for which the width W depends on r . Subsequently the time coordinate is converted to a

spatial coordinate by multiplying with the velocity, $w(x,y)$.

For the ST geometry the above approximation is less accurate since the considered diffusion is perpendicular to the axis of the tube. Thus Eq. (4) is converted to the 2D pseudo transient equation:

$$\frac{w(x,y)\tau}{L} \frac{\partial C_i}{\partial t'} - D_i \left(\frac{\partial^2 C_i}{\partial x^2} + \frac{\partial^2 C_i}{\partial y^2} \right) = R_i \quad (24)$$

where velocity $w(x,y)$ is obtained from the Poiseuille tube equation and t' is a time related to the z component defined as:

$$t' = \frac{z}{L} \tau. \quad (25)$$

Thanks to these previous considerations the 3D approach can be converted into 2D transient approach

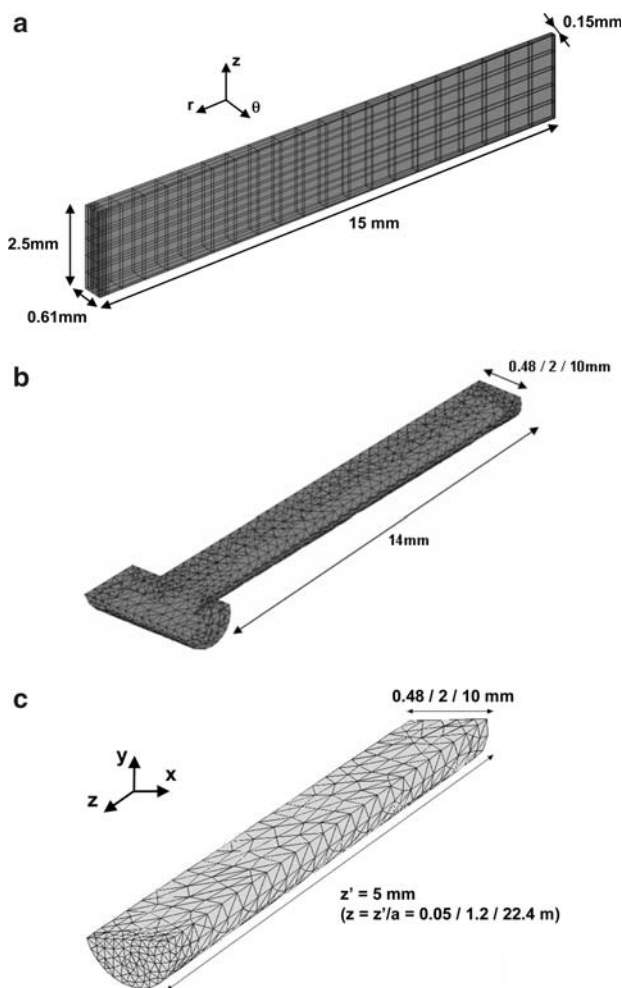


Fig. 2 **a** Mesh used for the 3D simulations of SFIMM; **b** mesh used for the 3D simulations of TJ; **c** mesh used for the 3D simulations of ST

when $Pe_L \gg 1$. This leads to a tremendous reduction of the computing time while decreasing the required storage memory. Furthermore the mesh of the 2D section is much finer compared to the (x,y) section of the 3D mesh especially where strong variations in reagent concentrations are likely to occur. Moreover, all 2D model equations have been rewritten in a dimensionless form to help in a rapid study of different microreactors dimensions. Thus, the subsequent normalized meshes are, respectively, half of a circle for the ST and a rectangle for the SFIMM (cf. Fig. 4).

In addition, calculations on a finer mesh have been performed for both 3D and 2D meshes but did not lead to more than 2% discrepancy with the mesh used for all the presented simulations.

5 Results and discussion

To ensure the best control over the polymerization two conditions have to be simultaneously fulfilled (1) the mixing must be good enough to avoid local chemical species concentration fluctuations, (2) there must be no temperature gradient within the reactor. If one of these conditions is not fulfilled a broadening of the molecular weight distribution and thus an increase in the polydispersity index are observed. Then to determine the microreactor which allows the best control over the polymerization, two different types of numerical simulations were performed: concentration field and polymerization, for which operating conditions are given in Table 2.

5.1 Concentration field

The degree of mixing achieved in each microreactor can be assessed by studying the relative concentration of styrene in the exits section of the devices (ST and SFIMM). The relative concentration is defined as C_M/C_{M0} . Thus $C_M/C_{M0} = 100\%$ corresponds to pure styrene while $C_M/C_{M0} = 0\%$ means that there is only solvent. The concentration field is calculated by running the simulations without taking into account the polymerization reaction. The operating conditions and devices' volumes were identical to those required for the polymerization, i.e. a mean residence time of 12 h and a temperature of 70°C. Thus, styrene and solvent flowrates are fixed accordingly to the microreactors' volumes (cf. Table 2). For the tubular reactor, the concentration field is obtained in two steps. The first step consists in getting the styrene relative concentration in the exit section of the TJ by using the mesh depicted in Fig. 2b. Then, this relative concentration

Table 2 Operating conditions

	SFIMM	TR 0.24	TR 1	TR 5
Concentration field simulations				
Styrene flowrate (μl/min)	3.82	–	–	3.82
Solvent flowrate (μl/min)	1.64	–	–	1.64
Wall temperature (°C)	70	–	–	70
Chemical species diffusion coefficient (m ² /s)	4 × 10 ⁻¹³ and 10 ⁻¹¹	–	–	8 × 10 ⁻¹¹ and 2 × 10 ⁻⁹
Radial Peclet number (–)	5.38 and 0.21	–	–	5.65 and 0.22
Polymerization simulations				
Mean residence time (h)	12	12	12	12
Styrene flowrate (μl/min)	3.82	3.82	3.82	3.82
Solvent flowrate (μl/min)	1.64	1.64	1.64	1.64
Initiator to monomer mass ratio	0.40%	0.40%	0.40%	0.40%
Wall temperature (°C)	70	70	70	70
Initiator (AIBN) half-life time (h)	3	3	3	3
Chemical species diffusion coefficient (m ² /s)	4 × 10 ⁻¹³ to 10 ⁻⁸	2 × 10 ⁻¹³ to 10 ⁻⁸	3 × 10 ⁻¹² to 10 ⁻⁸	8 × 10 ⁻¹¹ to 10 ⁻⁸
Axial Peclet number (–)	1.12 × 10 ⁶ to 4.48 × 10 ¹	5.81 × 10 ¹⁰ to 1.16 × 10 ⁶	1.21 × 10 ⁷ to 3.63 × 10 ³	7.23 × 10 ² to 5.79
Radial Peclet number (–)	5.38 to 2.15 × 10 ⁻⁴	6.47 to 1.29 × 10 ⁻⁴	7.72 to 2.31 × 10 ⁻³	5.65 to 4.52 × 10 ⁻²

field is used as the inlet boundary condition for the ST section using the mesh depicted in Fig. 2c.

Figures 5a and 6a give the 3D relative concentration of styrene, respectively, for SFIMM and TR 5, and for low radial Peclet numbers. Here, the radial Peclet number is defined as the ratio of the characteristic time of diffusion in the direction perpendicular to the main flow to the characteristic time of convection in the flow direction and is expressed as follows for each device:

$$Pe_R(\text{TR}) = \frac{Q}{\pi D L_{\text{TR}}} \tag{26}$$

$$Pe_R(\text{SFIMM}) = \frac{(W_0/2)^2}{D \tau} \tag{27}$$

where Q denotes the total flow rate, $L_{\text{TR}} = L_{\text{TJ}} + L_{\text{ST}}$ the sum of the TJ and ST section lengths (14 + 50 mm for TR 5) and W_0 the width at the entry of the SFIMM trapezoidal cut (0.61 mm, cf. Fig. 2a). For these radial

Peclet numbers (0.21 and 0.22, respectively), both devices exhibit a very good mixing as proved by the homogeneous orange color at the exits corresponding to $C_M/C_{M0} = 70\%$. Indeed this value corresponds to the styrene to the solvent flowrates ratio. However, the SFIMM’s radial Peclet number is obtained with a diffusion coefficient two decades lower than that of the TR 5 (10⁻¹¹ and 2 × 10⁻⁹ m² s⁻¹, respectively). It results directly from the significant reduction in the characteristic length of the SFIMM ($W_0/2$) compared to TR 5 (R).

As the diffusion coefficient decreases, the TR 5 exhibits a poor mixing. However, it is worthwhile to note that for much lower diffusion coefficients the SFIMM gives a better mixing than the TR 5 (cf. Figs. 5b, 6b). Indeed the styrene relative concentration at the exit of the SFIMM ranges from 60 to 78% for a diffusion coefficient value of 4 × 10⁻¹³ m² s⁻¹ while for a diffusion coefficient of 8 × 10⁻¹¹ m² s⁻¹ the relative

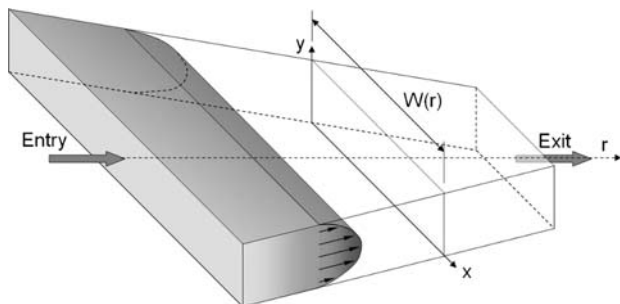


Fig. 3 Sketch of the flow between parallel plates for the SFIMM subjected to convection and diffusion

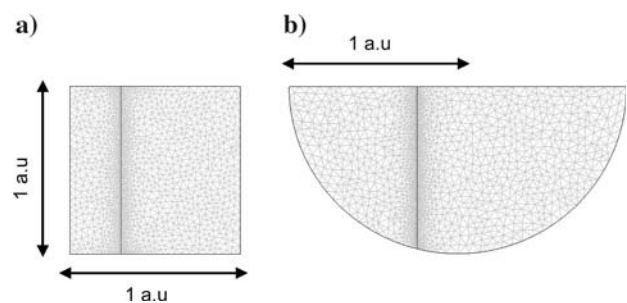


Fig. 4 Meshes used for the 2D simulations of a SFIMM, b ST

concentration at the TR 5's exit still ranges from 0 to 100%.

Globally, it should be noticed that the smaller the characteristic length, the smaller is the diffusion coefficient for which one can get a styrene relative concentration of 70%. This means that TRs with very small radii can achieve even better mixing than the SFIMM as shown in the next polymerization section.

To validate the use of the 2D model, the 3D relative concentration of styrene at the exit of the ST section has been compared with that returned by the 2D model for two different diffusion coefficients (cf. Fig. 7). As seen there is a fairly good agreement between the 3D and 2D models. The same conclusion holds also for the SFIMM microreactor. Therefore the 2D model was used where the polymerization takes place. Then the whole SFIMM was modeled with the 2D model while only the ST section of the tubular reactor was modeled with the 2D model. For the ST section, the 2D initial conditions correspond to the exit concentration fields returned by the 3D simulation of the TJ section. It should be recalled that the TJ section is kept at a low temperature so that no polymerization occurs in that section.

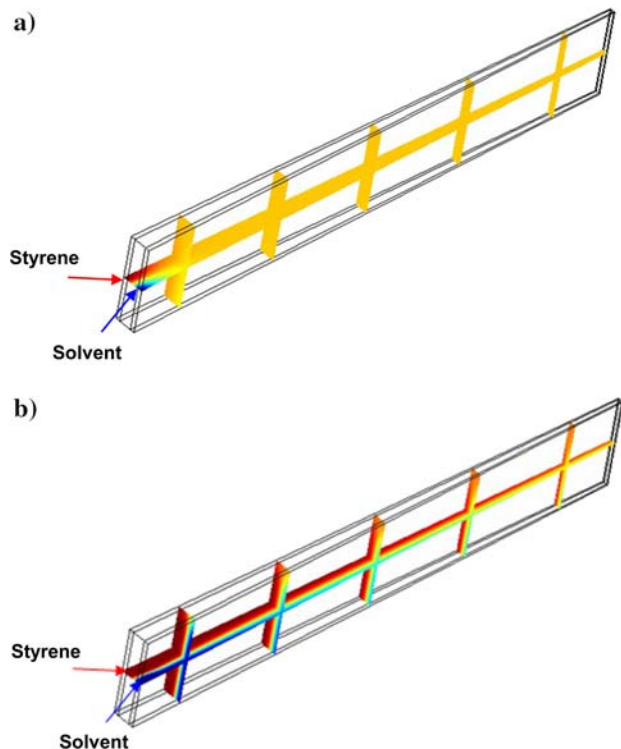


Fig. 5 SFIMM's styrene relative concentration for **a** $D = 10^{-11} \text{ m}^2 \text{ s}^{-1}$ and **b** $D = 4 \times 10^{-13} \text{ m}^2 \text{ s}^{-1}$ (blue $C_M/C_{M0} = 0\%$; red $C_M/C_{M0} = 100\%$)

5.2 Polymerization

The numerical simulations of the styrene free radical polymerization were directly performed in the focusing section of the SFIMM and in the ST section of the tubular reactor. The wall temperature was set to 70°C for both microreactors. For these simulations, the operating conditions are given in Table 2. We did not take into account the change in the fluid viscosity with respect to the temperature and the reaction yield. Indeed, due to the high wall surface to volume ratio encountered in microfluidic devices, the temperature does not change significantly and thus would not affect the viscosity. Nevertheless, we have investigated the influence of the diffusion coefficient which was assumed to be identical for all chemical species. However, a decrease in the diffusion coefficient can reflect an increase in the medium viscosity.

The simulations show that, despite the heat released by the polymerization, there is almost no temperature variation in the microreactor. Indeed, the simulations indicate a difference smaller than 0.1°C between the wall surface and the heart of the SFIMM or the center of ST. It results from the high value of the wall surface to volume ratio (cf. Table 1) exceeding by several orders of magnitude, the ratio usually encountered in laboratory or industrial equipments.

The influence of the chemical species diffusion coefficient (D_i) on the macromolecular weight distribution obtained in the SFIMM and TRs is given in Fig. 8. One can observe that both SFIMM and TRs follow the same trend. As expected, when the diffusion coefficient increases, the PDI tends to the theoretical limiting value of 1.5 encountered for a free radical polymerization with combination termination in an

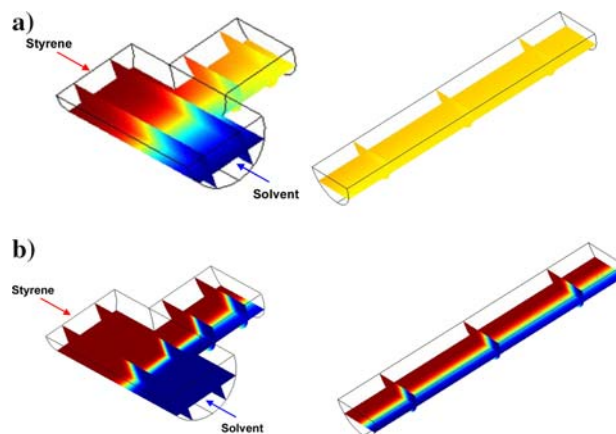
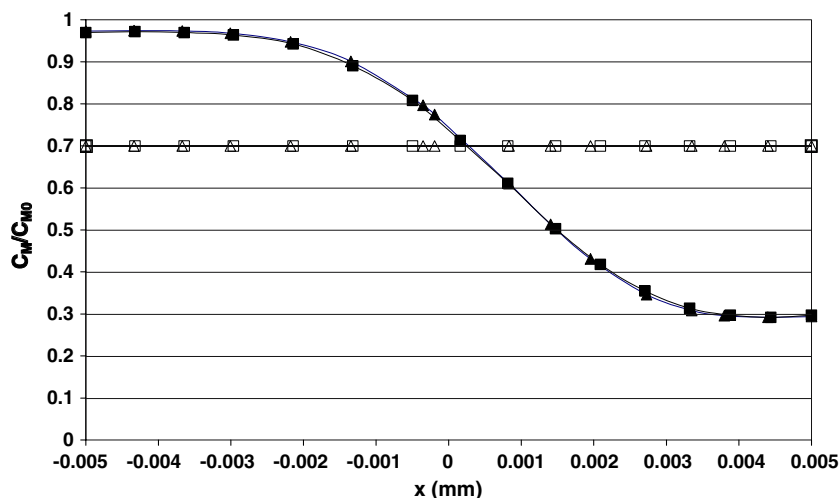


Fig. 6 TJ 5 (left) and ST 5 (right) styrene relative concentration for **a** $D = 2 \times 10^{-9} \text{ m}^2 \text{ s}^{-1}$ and **b** $D = 8 \times 10^{-11} \text{ m}^2 \text{ s}^{-1}$ (blue $C_M/C_{M0} = 0\%$; red $C_M/C_{M0} = 100\%$)

Fig. 7 Relative monomer concentration at the exit of ST 5 for the 3D model (filled square) and 2D model (filled triangle). $D = 8 \times 10^{-11} \text{ m}^2 \text{ s}^{-1}$ (filled symbols) and $D = 2 \times 10^{-9} \text{ m}^2 \text{ s}^{-1}$ (open symbols)



ideal batch or plug flow tube reactor. On the other hand, when the diffusion coefficient decreases one observes a rather sharp increase in the polydispersity index. It is believed that this is mainly due to a broadening of the residence time distribution (RTD). However, the smaller the tube reactor radius, the smaller is the diffusion coefficient for which this sharp increase in PDI occurs. This practically means that by using tube reactors with radii in the range of hundreds of micrometers rather than laboratory or industrial scale tube reactors, one can get a good control all over the polymerization despite the continuous increase in medium viscosity resulting from the monomer conversion. It is worthwhile to note that the SFIMM curve has exactly the same shape than the TRs curves. Therefore additional simulations were performed to determine the tubular reactor radius for which the PDI curve will superimpose to the SFIMM one. So, it was found that the SFIMM acts like an equivalent tubular reactor of 0.39 mm radius and 8.3 m length. However, it should be emphasized that due to its very compact geometry, the SFIMM leads to much less pressure drop than its equivalent tubular reactor. The pressure drop ratio between the equivalent tubular reactor and SFIMM has been analytically found higher than 10^8 (!).

Figure 9 gives the variation of the monomer conversion (X_M) with the diffusion coefficient. One observes that as the diffusion coefficient decreases, the monomer conversion is first kept constant close to the value of 73% and then rapidly decreases. It simply results from the mixing efficiency which falls down as the diffusion coefficient decreases. Moreover, as the tube radius decreases, the monomer conversion is kept to the highest value of 73% on a wider range of diffusion coefficients. This can be explained by the time

required to homogenize the reactive media which decreases as the tube radius decreases.

The last interesting parameter is the number-average degree of polymerization (DP_n) which variation with respect to the diffusion coefficient is reported in Fig. 10. As the diffusion coefficient decreases, the DP_n starts to slightly decrease and then sharply increases. Actually, this behavior reflects the competition between two opposite phenomena. On one hand, when the diffusion coefficient decreases, the propagation reaction becomes diffusion-controlled. The polymerization rate decreases, less monomer is incorporated in the macromolecular chains resulting in a decrease in the DP_n . On the other hand, when the diffusion coefficient is too low, the reaction medium cannot be homogenized by the diffusion phenomenon. Then, the polymerization reaction can occur only at the fluid interphase where concentrations of chemical species are the highest. This highly favors the propagation reaction resulting in a rapid incorporation of the monomer.

6 Conclusions

The styrene free radical polymerization performed in two types of lamination microreactor was investigated by means of 2D and 3D finite elements numerical simulations. For high axial Peclet numbers, it was found that the 2D model gives a fairly good agreement with the 3D model. In addition to reduce the memory required for the simulations, the 2D model allows to adapt the mesh refinement where high gradients of reagents concentrations occur. It was also found that despite the heat released by the polymerization, the thermal transfer in such microfluidic devices is high

Fig. 8 Variations of the polydispersity index (*filled triangle* SFIMM; *open circle* TR 0.24; *filled diamond* TR 1; *filled square* TR 5)

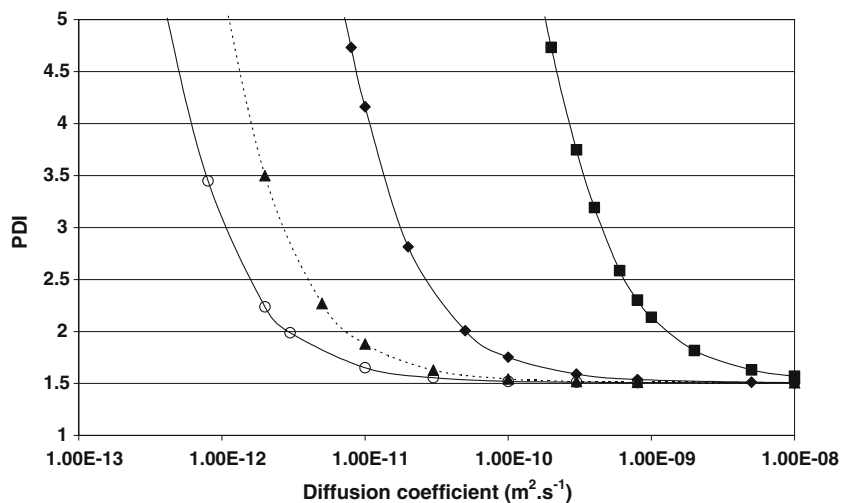


Fig. 9 Variations of the monomer conversion (*filled triangle* SFIMM; *open circle* TR 0.24; *filled diamond* TR 1; *filled square* TR 5)

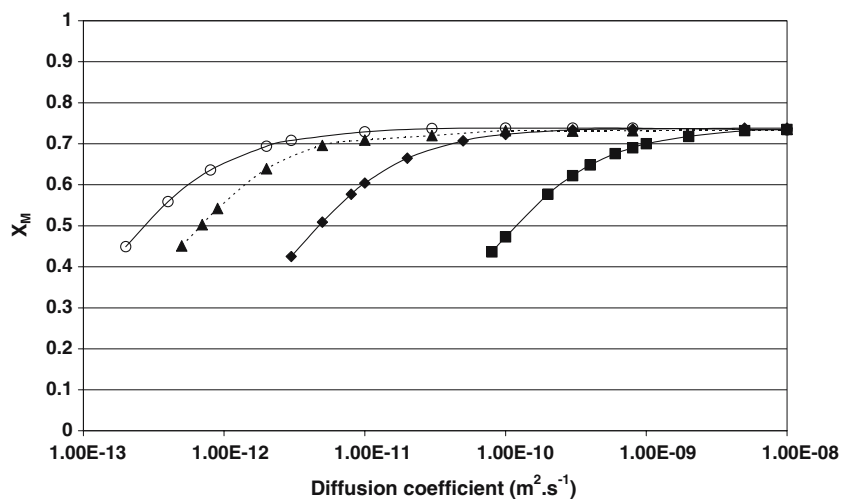
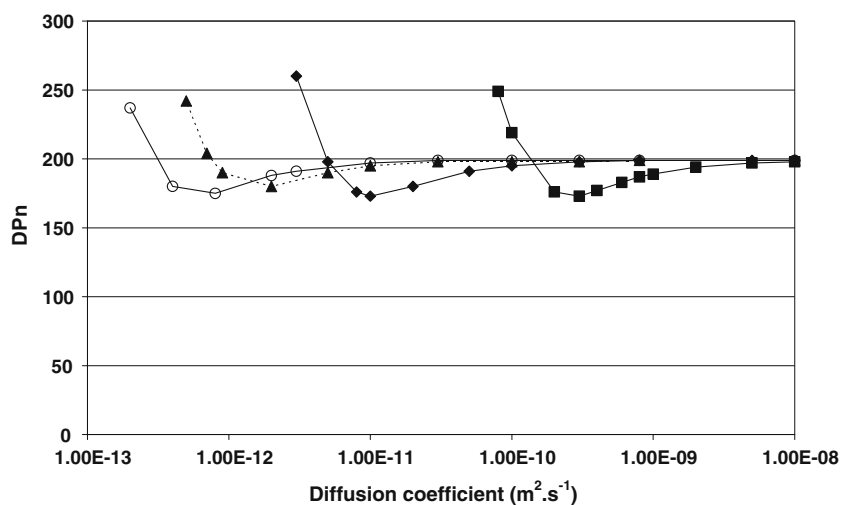


Fig. 10 Variations of the number-average degree of polymerization (*filled triangle* SFIMM; *open circle* TR 0.24; *filled diamond* TR 1; *filled square* TR 5)



enough to ensure isothermal conditions. The multiamination interdigital microreactor and tubular reactors with radii of hundreds of micrometers allow

keeping the PDI close to the theoretical limiting value of 1.5 over a large range of diffusion coefficients. However, as the tube radius increases, one loses the

control over the polymerization, and the PDI gets higher than 1.5. This is typically the case for laboratory and industrial scale reactors. It was also found that the SFIMM acts as an equivalent tubular reactor of 0.39 mm radius and 8.23 m length. However, due to its shorter length, the SFIMM induces less pressure drop which therefore makes it suitable for the flow of highly viscous fluids. Furthermore it can be easily cleaned up in case of fouling.

In conclusion, the simulations show that the use of microfluidic devices can achieve a better control over the free radical polymerization than macroscale reactors.

Acknowledgments C.S. thanks the French Ministry of Higher Education and Research for supporting this work through the special grant dedicated to young researchers: ACI “Jeunes Chercheurs et Jeunes Chercheuses” no. JC8075. The authors also thank the IMM Company for having provided all the SFIMM characteristics as well as for their valuable discussions about their systems.

References

- Bayer T, Pysall D, Wachsen O (2000) Micro mixing effects in continuous radical polymerization. In: Ehrfeld W (ed) *Microreaction technology: 3rd International Conference on Microreaction Technology*, Springer, Berlin Heidelberg New York
- Cabral JT, Hudson SD, Wu T, Beers KL, Douglas JF, Karim A, Amis EJ (2004) Microfluidic combinatorial polymer research. In: *Proceedings of the American Physical Society March meeting 2004*, Montreal (Canada), March 22–26, 2004
- Chen CC (1998) Simulation of a continuous bulk styrene polymerization process with catalytic initiation for crystal-clear polymer and rubber-modified polystyrene. *Polym Reac Eng* 6(3–4):145–192
- Dostson NA, Galván R, Laurence RL, Tirrell M (1996) *Polymerization process modeling*. Wiley-VCH, Weinheim
- Geschke O, Klank H, Telleman P (2004) *Microsystem engineering of lab-on-a-chip devices (biotechnology: a multi-volume comprehensive treatise)*, 2nd edn. Wiley, New York
- Hessel V, Löwe H (2005) Micro mixers—a review on passive and active mixing principles. *Chem Eng Sci* 60:2479–2501
- Hessel V, Hardt S, Löwe H (2004) *Fundamentals, modelling and reactions, in chemical micro process engineering*. Wiley-VCH, Weinheim
- Hessel V, Serra C, Löwe H, Hadziioannou G (2005) Polymerisationen in mikrostrukturierten reaktoren: ein überblick. *Chem Ing Tech* 77:1693–1714
- Hisamoto H, Saito T, Tokeshi M, Hibara A, Kitamori T (2001) Fast and high conversion phase-transfer synthesis exploiting the liquid–liquid interface formed in a microchannel chip. *Chem Comm* 24:2662–2663
- Honda T, Miyasaki M, Nakamura H, Maeda H (2005) Controllable polymerization of *N*-carboxy anhydrides in a microreaction system. *Lab Chip* 5(8):812–818
- Iedema PD, Grcev S, Hoefsloot HCJ (2003) Molecular weight distribution modeling of a radical polymerization in a CSTR with long chain branching through transfer to polymer and terminal double bond (TDB) propagation. *Macromolecules* 36:458–476
- Iwasaki T, Yoshida (2005) Free radical polymerization in microreactors. significant improvement in molecular weight distribution control. *Macromolecules* 38(4):1159–1163
- Liu S, Chang C-H, Paul BK, Remcho VT, Abhinkar B (2006) Synthesis of dendrimers using continuous flow microreactors. In: *Proceedings of 2006 AIChE spring national meeting, Orlando (USA)*, 22–27 April 2006
- Miyazaki M, Honda T, Nakamura H, Maeda H (2006) Amino acid polymerization in micro-reactor. In: *Proceedings of 2006 AIChE spring national meeting, Orlando (USA)*, 22–27 April 2006
- Nagaki A, Kawamura K, Suga S, Ando T, Sawamoto M, Yoshida J (2004) Cation pool-initiated controlled/living polymerization using microsystems. *J Am Chem Soc* 126:14702
- Rosenfeld C, Serra C, Brochon C, Hadziioannou G (2006a) Use of micro mixers to control the molecular weight distribution in continuous two-stage nitroxide-mediated copolymerizations. In: *Proceedings of the 9th international conference on microreaction technology, Potsdam (Germany)*, 6–8 September 2006
- Rosenfeld C, Serra C, Brochon C, Hadziioannou G (2006b) High temperature nitroxide-mediated radical polymerization in a continuous microtube reactor: towards a better control of the polymerization reaction. In: *Proceedings of the 19th international symposium on chemical reaction engineering, Potsdam (Germany)*, 3–6 September 2006
- Villiermaux J, Blavier L, Pons M (1983) A new method for modelling free radical polymerization and predicting polymer quality In: Reichert KH, Geissler W (eds) *Polymer reaction engineering* Hanser, New York, pp 3–20
- Wong SH, Ward MCL, Wharton CW (2004) Micro T-mixer as a rapid mixing microreactor. *Sens Actuators B Chem* 100(3):365–385
- Wu T, Mei Y, Cabral JT, Xu C, Beers KL (2004) A new synthetic method for controlled polymerization using a microfluidic system. *J Am Chem Soc* 126(32):9880–9881
- Wu T, Mei Y, Xu C, Byrd HCM, Beers KL (2005) Block copolymer PEO-b-PHPMA synthesis using controlled radical polymerization on a chip. *Macromol Rapid Commun* 26(13):1037–1042
- Zhu S (1999) Modeling of molecular weight development in atom transfer radical polymerization. *Macromol Theor Simul* 9:29–37